Approaches for measuring the surface areas of metal oxide electrocatalysts for determining their intrinsic electrocatalytic activity

Wei, Chao; Sun, Shengnan; Mandler, Daniel; Wang, Xun; Qiao, Shi Zhang; Xu, Zhichuan Jason

2019

Wei, C., Sun, S., Mandler, D., Wang, X., Qiao, S. Z. & Xu, Z. J. (2019). Approaches for measuring the surface areas of metal oxide electrocatalysts for determining their intrinsic electrocatalytic activity. Chemical Society Reviews, 48(9), 2518-2534. https://dx.doi.org/10.1039/c8cs00848e

https://hdl.handle.net/10356/153350

https://doi.org/10.1039/c8cs00848e

Approaches for measuring surface area of metal oxide electrocatalysts for determining the intrinsic electrocatalytic activity

Received 00th January 20xx,
Accepted 00th January 20xx

DOI: 10.1039/x0xx00000x

www.rsc.org/

Chao Wei,[a] Shengnan Sun,[a] Daniel Mandler,[bc] Xun Wang,[d] Shi Zhang Qiao[e] and Zhichuan J. Xu*[acfg]

A great interest has been recently drawn to the metal oxide electrocatalysts for electrocatalysis-based energy storage and conversion devices. To find the optimal electrocatalyst, the prerequisite is an activity metric that reasonably evaluates the intrinsic electrocatalytic activity. The intrinsic activity is commonly defined as the specific activity being the current per catalyst surface area. Thus, the precise assessment of intrinsic activity highly depends on the reliable measurement of catalyst surface area, which calls for the knowledge of experimental approaches for determining the surface area of metal oxide electrocatalysts. This tutorial review aims to summarize and analyze the approaches for measuring the surface area of metal oxide electrocatalysts for evaluating and comparing the intrinsic electrocatalytic activity. We start from comparing the popular metrics for activity estimation and highlighting the importance of surface-area-normalized activity (i.e. specific activity) for intrinsic chemistry analysis. Second, we provide some general guidelines for experimentally measuring the electrochemical active surface area (ECSA). Third, we review the methods for surface area measurement of metal oxide electrocatalysts. The detailed procedures for each method is explicitly described to provide a step-by-step manual that guides researchers to perform the measurement; the rationales and uncertainties for each method are discussed to help readers justify the reliable assessment of surface area. Next, we give our recommendations on selecting a rational experimental approach for the surface area measurement of a particular metal oxide electrocatalyst. Lastly, we discuss the future challenges of ECSA measurement and present an exemplary novel ECSA technique.

1. Introduction

The climate changes and the scarcity of fossil fuels have stimulated great interest on the electrocatalysis-based renewable energy devices with H_2 as the energy carrier, such as water electrolyzers and fuel cells.[1,2] The elementary processes of these devices, including oxygen reduction reaction (ORR), oxygen evolution reaction (OER), hydrogen evolution reaction (HER) and hydrogen oxidation reaction (HOR), have motivated a large number of publications in recent years.[2] The leading target of studying these elementary reactions is inventing highly active electrocatalysts, which are the key to achieving high efficiency of energy storage and conversion. In order to find the optimal electrocatalyst, a prerequisite is establishing a correct and convenient activity metric that reasonably evaluates the electrocatalytic performance of a particular catalyst. Because electrocatalysis is in essence a surface reaction, where the adsorption/desorption of reactants/products take place only at or near the catalyst surface region, the intrinsic electrocatalytic activity is most frequently defined as the specific activity being the current divided by the surface area of the catalyst (e.g., $mA/cm^2_{catalyst}$).[3] Thus, the accurate measurement of catalyst surface area governs the reliable assessment of specific activity, and such a vital role of catalyst surface area necessitates sound experimental approaches for determining the surface area of catalysts.

This tutorial review aims to summarize and analyze the approaches for measuring the surface area of metal oxide-based electrocatalysts for evaluating and comparing the intrinsic electrocatalytic activity. Despite a variety of techniques for surface area measurement, it is widely accepted that the best way to extract specific activity is using the surface area measured by electrochemistry method, also known as electrochemical active surface area (ECSA). In ECSA measurement of various electrocatalysts, measuring the ECSA of metal is the most sophisticated, because of the simplicity and versatility of metal surface, which is capable of adsorbing various species. That capability at metal surface allows us to measure the ECSA via some characteristic adsorption reactions, such as H adsorption/desorption,[4] CO stripping,[5] underpotential deposition[6] and surface redox reaction.[7] The ECSA measurement of metal has been systematically studied by previous seminal reviews and articles.[8-10] However, ECSA measurement is still a challenge for other sets of electrocatalysts, including metal oxides, which have been recently receiving increasing attention in electrocatalysis, especially OER[2] and ORR.[2,3] The oxide surface is more complicated and less versatile than metal surface. Due to the limited capability of adsorbing species at oxide surface, the characteristic adsorption reaction for ECSA measurement of metal oxide is merely reported. At present, there is still a lack of articles that summarize or review the experimental methods for quantifying the surface area of metal oxides. To supplement this area, here we focus on metal oxide electrocatalysts and discuss the experimental methodologies for surface area measurement, including ECSA and other non-electrochemistry techniques.

[a] *School of Materials Science and Engineering, Nanyang Technological University, 50 Nanyang Avenue, 639798, Singapore. Email: xuzc@ntu.edu.sg*
[b] *Institute of Chemistry, The Hebrew University of Jerusalem, Jerusalem 9190401, Israel.*
[c] *Singapore-HUJ Alliance for Research and Enterprise (SHARE), Nanomaterials for Energy and Energy-Water Nexus (NEW), Campus for Research Excellence and Technological Enterprise (CREATE), Singapore 138602, Singapore.*
[d] *Key Lab of Organic Optoelectronics and Molecular Engineering, Department of Chemistry, Tsinghua University, Beijing, China.*
[e] *School of Chemical Engineering, The University of Adelaide, Adelaide, South Australia 5005, Australia.*
[f] *Solar Fuels Laboratory, Nanyang Technological University, 50 Nanyang Avenue, 639798, Singapore.*
[g] *Energy Research Institute @ Nanyang Technological University, 50 Nanyang Avenue, 639798, Singapore.*
Electronic Supplementary Information (ESI) available: Fig. S1 and S2. See DOI: 10.1039/x0xx00000x

In this tutorial review, to raise the electrochemical energy materials community's awareness of the pivotal role of surface area determination, we begin by comparing the popular metrics for activity estimation, highlighting the importance of surface-area-normalized activity (i.e. specific activity) for intrinsic chemistry analysis. Secondly, we provide some general guidelines for measuring the ECSA. We rationalize the use of a three-electrode cell, the selection of a reference electrode, the importance of gas inlet, and discuss the preparation of the working electrode. Thirdly, to facilitate the understanding of ECSA measurement, we briefly introduce the mechanism of ECSA methods at metal surfaces, which have laid the foundation for measuring the ECSA of metal oxides. Then we focus on the methods for surface area measurement of metal oxide (the priority of this review), where we demonstrate that the ECSA quantification is still challenging and at present we mostly rely on some non-electrochemistry techniques including atomic force microscopy (AFM), Brunauer-Emmett-Teller (BET) and electron microscopy. The detailed procedures for each method is explicitly described to provide a step-by-step manual that guides researchers to perform the experiment; the rationales and uncertainties for each method are discussed to help readers justify the reliable assessment of surface area, which consequently governs the accurate estimation of specific activity. Next, we give our recommendations on selecting a rational experimental approach for the surface area measurement of a particular metal oxide electrocatalyst. Lastly, we discuss the perspective to identify the future challenges that lie in the ECSA measurement and present an exemplary novel technique that measures ECSA by adsorption capacitance.

2. The need for surface area determination

In this section, we discuss the underlying rationales of each activity metric to guide the researchers to choose the correct activity metric according to the purpose of the conducted study; and we especially highlight the importance of specific activity in intrinsic activity studies. Currently, the most popular four metrics for describing the electrocatalytic activity are: geometric activity being the current density normalized to the geometric area of electrode (e.g., mA/cm^2_{geo} to reach a given potential; the overpotential at a given mA/cm^2_{geo}), mass activity being the current per loading mass of electrocatalysts (e.g., $A/g_{catalyst}$ at a given potential), turnover frequency (the number of electrons produced/consumed per active sites per second), and specific activity being the current per real surface area of electrocatalyst (e.g., $mA/cm^2_{catalyst}$ at a given potential). Three of them are schematically illustrated in Fig. 1a to visualize the differences.

Geometric activity is a practical parameter for evaluating the device performance, rather than for reflecting the intrinsic activity of electrocatalysts. Geometric activity is defined as the current density normalized to the geometric area of electrode. The energy community widely uses two parameters to describe the geometric activity: the overpotential to reach the geometric current density of 10 mA/cm^2 (denoted as η@10 mA/cm^2_{geo}),[11,12] which is the approximate current density expected in a 10% efficient integrated solar-to-fuels device under 1 sun illumination;[11] and the half-wave-potential, which is frequently used for ORR, sometimes alcohol oxidation. For the detailed historical origin of η@10 mA/cm^2_{geo} and its practical importance to device design (rather than catalyst design), we refer readers to a previous review.[12] Despite the practical significance of η@10 mA/cm^2_{geo} in the solar fuel application, we caution that geometric activity does not reflect the intrinsic activity of a given catalyst. The geometric activity fails to consider that the electrocatalytic reaction is a surface process, where only the surface sites participate in the reaction. On the other hand, the geometric activity is largely dominated by the loading mass of catalysts. It has been commonly observed that, with more catalysts loaded on the current collector, the overpotential to reach the given geometric-surface-area-normalized current density (denoted as i_{geo}) certainly becomes smaller; and i_{geo} at the given overpotential is higher.[12-14] For example, as shown in Fig. 1b, the catalyst loading effect on η@5 mA/cm^2_{geo} is scrutinized by OER at $La_{0.7}Ba_{0.15}Sr_{0.15}Co_{0.8}Fe_{0.2}O_{3-\delta}$ (50 nm) perovskite catalyst.[13] A larger catalyst loading moves the OER polarization curve towards the negative direction, and η@5 mA/cm^2_{geo} becomes smaller. Another example is OER at IrO_2,[11,12] where η@10 mA/cm^2_{geo} decreases with increasing catalyst loading. The same catalyst loading dependence of geometric activity is also reported for OER i_{geo}@1.6 V vs. RHE, which increases with a larger loading of perovskites (including $Ba_{0.5}Sr_{0.5}Co_{0.8}Fe_{0.2}O_{3-\delta}$, $La_{0.6}Sr_{0.4}Co_{0.2}Fe_{0.8}O_{3-\delta}$ and $Pr_{0.5}Ba_{0.5}CoO_{3-\delta}$).[14] The other parameter for describing geometric activity, namely the half-wave-potential estimated by i_{geo}, is essentially the same as η@10 mA/cm^2_{geo}, and thus it has the same catalyst loading dependence. Increasing the catalyst loading shifts the half-wave potential towards the low-overpotential direction. We thus warn researchers that since various publications use different loading mass, the activity comparison across the literatures, in terms of geometric activity such as η@10 mA/cm^2_{geo} or half-wave-potential, does not necessarily reflect the intrinsic chemistry of the catalyst. The seemingly different activity in the metric geometric activity might be simply due to the various catalyst loading, rather than the intrinsic electrochemical performance of the catalyst.

Mass activity largely depends on the size of electrocatalyst particles (i.e. the number of active sites) and it is unable to represent the intrinsic electrocatalytic activity. Mass activity is obtained by normalizing the current density to the loading mass of

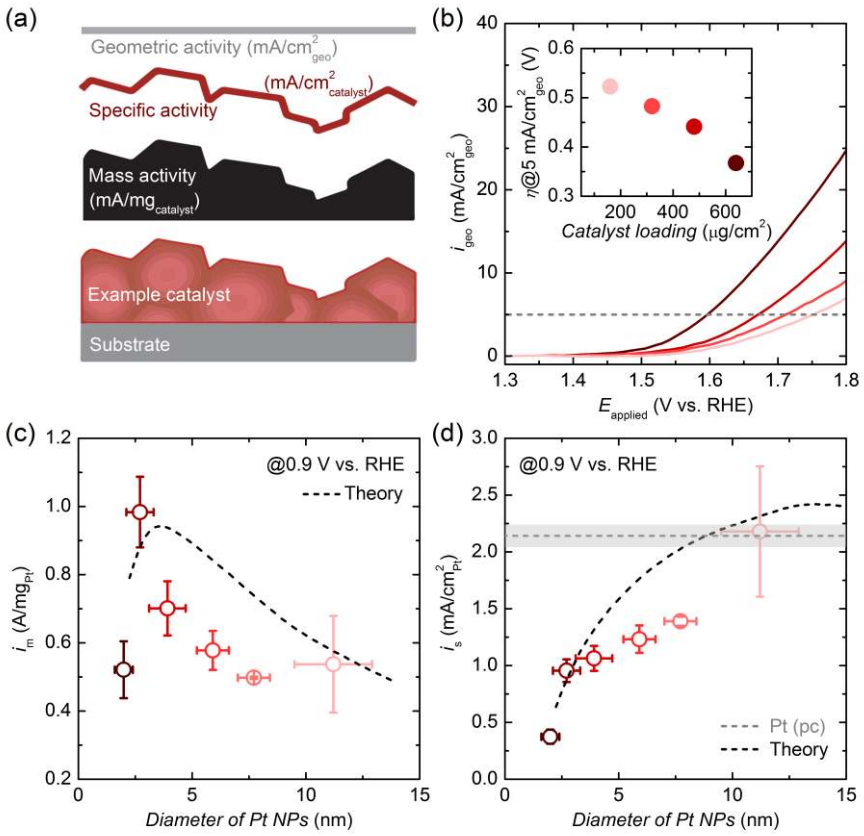

Fig. 1 (a) A model catalyst surface[15] that visualizes the definition of geometric activity (normalized to the projected geometric area of electrode), specific activity (normalized to the surface area of catalyst) and mass activity (normalized to the loading mass of catalyst), necessitating the surface area and active site normalized metric of activity for comparing the intrinsic performance of catalysts. Reproduced from ref. [15] with permission from Springer Nature, copyright 2016. (b) The background-corrected OER polarization curves with various loading mass of $La_{0.7}Ba_{0.15}Sr_{0.15}Co_{0.8}Fe_{0.2}O_{3-\delta}$-50 nm catalyst,[13] demonstrating the geometric activity depends on the loading mass of catalyst. The polarization curve is collected at a scan rate of 10 mV/s and rotation speed of 1600 rpm in O_2-saturated 0.1 M KOH. Inset is the OER overpotential@5 mA/cm$^2_{geo}$ as a function of catalyst loading mass. Reproduced from ref. [13] with permission from Royal Society of Chemistry, copyright 2016. (c) ORR mass activities and (d) specific activities at mass-selected Pt nanoparticles (NPs) versus their particle sizes.[16] The black dash lines are theoretical trends estimated by simulation and the gray dash line is the specific activity of polycrystalline Pt, denoted as Pt (pc). (c and d) are reproduced from ref. [16] with permission from John Wiley and Sons, copyright 2012.

the electrocatalysts. The mass activity may serve as a reasonable parameter for evaluating intrinsic performance of different electrode materials in bulky chemistry processes, such as lithium-ion battery reactions, where the Li^+ diffuses deeply into the material and the original micro-structure cracks with charge/discharge cycles.[17] However, for the surface chemistry processes such as electrocatalysis and even supercapacitor, where the reaction occurs only at/near the surface and the electrode materials normally possess better bulky structural stability, the mass activity does not represent the intrinsic activity.[3] It reflects more the cost efficiency of given catalysts using the same materials, i.e. the mass activity of Pt and Pt-based catalysts is an indicator of the Pt cost and meaningful in an engineering perspective. The definition of mass activity assumes that all atoms within each particle are electrocatalytic active sites, which is in conflict with the fact the interior atoms beneath the surface area do not contribute to the electrocatalytic process. As a result, the activity being per mass is largely dependent on the particle size (or equivalently, surface area of catalyst), which reflects the fraction of surface atoms. Usually, catalysts of smaller particle size give higher mass activity, because smaller sized particles possess a larger ratio of surface atoms to the total atoms per mass and give a larger number of electrocatalytic active sites. An example to demonstrate this mass activity-size relationship is the effect of particle size on ORR of mass-selected Pt (Fig. 1c),[16] where decreasing the size (particle diameter) from ~12 to ~3 nm results in an increasing ORR mass activity (i_m). The mass activity at <2.5 nm seems to be an exceptional case, which will be clarified later. This trend of mass activity as a function of size is also supported by that predicted from a simulation study (dash line, Fig. 1c).[16] Considering this size dependence, mass activity is of great engineering significance for estimating the practical performance and guiding the optimization of the volumetric size, weight and cost of electrochemical devices. However, mass activity cannot reveal the intrinsic chemistry difference of various electrocatalysts.

Turnover frequency (TOF) is the most reasonable description of intrinsic activity, but mostly difficult to assess. TOF is defined as the number of electrons produced/consumed per active site per second at a defined operation potential (for example, /s@0.9 V vs. RHE for ORR at Pt-based catalysts).[18] As indicated by the definition, the experimental extraction of TOF requires both the measurement of

current density, which is converted to the number of electron transfer, and the reliable assessment the number of active sites. The current density can be accurately measured by the present-day electrochemical workstation such as potentiostat. Unfortunately, due to the fact that the modern technology has limited ability to unambiguously measure the number of active sites, the accurate estimation of TOF is still a challenge. Up to date, the most popular method for obtaining TOF is to convert the surface area of electrocatalyst to the number of active sites via a coefficient that defines the number of surface atom being per surface area (e.g., /nm^2). However, this coefficient is usually determined by referencing the value from the literature. Directly using the reported value is, in essence, empirical and arbitrary, as the active site density at surface probably varies with each individual material, which might have different surface properties, such as surface orientation.[19] As an example, the density of active metal-site on the (100) surface of the rutile IrO_2 and RuO_2 are higher than on (110).[19] The TOF estimated via such empirical coefficient of surface atom density may serve as an important reference for screening the catalytic activity, but researchers are alerted to be cautious about the accuracy. Alternatively, the number of active site can be measured by cyclic voltammetry (CV), where the coulombic charge of the specified CV peak quantifies the atoms participating in the reaction. For example, the oxidation peak of Ni cations (~1.4 V vs. RHE) at $Ni_{0.8}Fe_{0.2}O_xH_y$ film is integrated and converted to the number of active metal cations assuming this is a one electron transfer redox.[1] However, this method is only applicable to materials that have clear pre-catalytic redox CV features. For example, in the class of metal oxides, only Ni- and Co-based metal oxides are promising candidates for such analysis.[1] Moreover, the uncertainty of this method originates from several assumptions such as the electron transfer number, the background subtraction for peak integration, etc. For more detailed analysis about the ambiguity and limitation of this method, we refer the readers to a seminal review.[1] It is also worth noting that, to obtain the TOF, some studies simply convert the mass loading of the catalyst to the number of active sites via the molecular weight. Such mass-based TOF is intrinsically equivalent to the mass activity, which assumes all atoms within the particle are active sites, and thus this metric does not reflect the intrinsic activity. To summarize, TOF is the intrinsic activity, but currently it is difficult to measure.

Specific activity represents the intrinsic activity. Specific activity is estimated by normalizing the current density to the surface area of electrocatalyst. Because surface area is associated with the number of surface atoms, which indicates the real number of active sites, the specific activity is actually a practical approximation of the activity per active site (TOF), and it reflects the intrinsic activity of chemistry. Up to date, due to the limited technology capability of characterizing the number of active sites, specific activity is the best alternative to TOF and considered as the universal activity metric for investigating intrinsic chemistry. Our preference to specific activity does not deny the guiding role of mass activity and geometric activity in engineering or industrial application. However, with the purpose of revealing the fundamental electrocatalytic mechanisms, especially in descriptor studies that reveal why different catalysts have different electrochemical performance,[3,20,21] this review aims to necessitate the employment of specific activity. We caution that if the analysis of the intrinsic chemistry is based on the geometric activity or mass activity, the conclusion possibly deviates from the truth and may confuse the researchers with limited experience in electrocatalysis.

Hereby, the rationales of each activity metric are discussed. To seize a better understanding of these activity metrics, we present a classic example, namely the effect of size on ORR activity of mass-selected Pt nanoparticles (NPs),[16] to help interpret the different insights that are brought by the different activity metrics. In terms of mass activity or geometric activity, the smaller sized Pt NPs give better performance (Fig. 1c),[16] because they have more surface atoms. This is exactly the reason for the real fuel cell industries to prefer nano-sized Pt NPs than bulky materials. However, the mass activity or geometric activity does not explain the phenomenon that mass activity reaches the maximum at the particle size of ~3 nm. In contrast, if we examine the intrinsic chemistry of the active sites, shrinking the particle size of Pt results in a smaller specific activity (Fig. 1d),[16] which indicates that the surface Pt atoms become less active. Although the electron transfer at the individual active site is slower, the larger fraction of surface atoms at smaller NPs enables the total current to grow. Thus, an increasing mass activity is observed. For size <2.5 nm, there is a quite large number of active sites, but as indicated by the specific activity metric, these surface Pt atoms are so less active that the mass activity drops. As exemplified by this size effect on various metrics of ORR activities at Pt, we recommend researchers to choose the correct activity metric according to the purpose of the conducted study. With the purpose of understanding the intrinsic chemistry of electrocatalyst, we rely on the analysis of specific activity, which calls for the experimental approaches for determining the surface area of catalysts.

3. General guidelines for measuring ECSA

This section provides general guidelines for measuring the ECSA of catalysts. We rationalize the use of three-electrode cell, the selection of reference electrode, importance of gas inlet, and discuss the preparation of the working electrode.

The ECSA measurement uses a three-electrode cell (as shown in Fig. 2a), which has a gas inlet, a reference electrode, a working

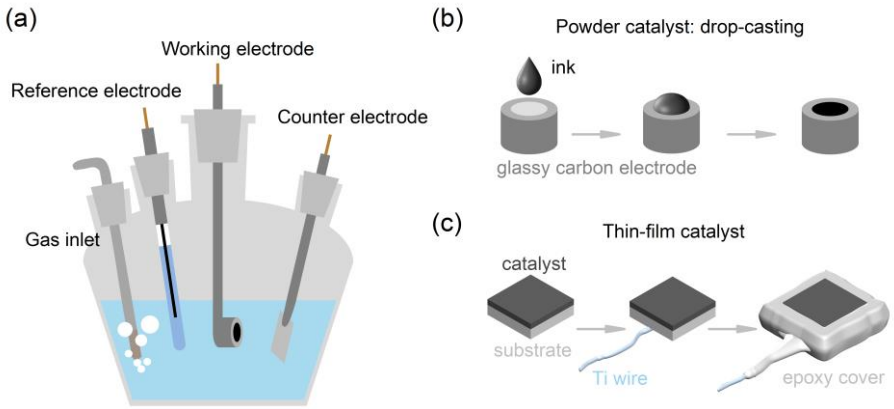

Fig. 2 (a) The schematic illustration of a typical three-electrode cell for ECSA measurement. The cell includes a gas inlet, reference, working and counter electrodes. (b) The exemplary step-wise procedures for working electrode preparation of powder catalysts. The exemplary working electrode is a Teflon-shrouded glassy carbon, where the powder catalysts are applied in the form of a uniform thin layer by the traditional drop-casting method. (c) The exemplary step-wise procedures for working electrode preparation of thin-film catalysts, which are intrinsically grown on the substrate. The substrate is attached with a Ti wire; and then covered with epoxy to only expose the active region.

electrode and a counter electrode. In order to accurately know the potential at the catalysts, the potential of the working electrode (where catalysts locate) needs to be measured/applied against a reference electrode, where the potential is well-defined. Therefore, for higher accuracy of potential control, ECSA measurement requires a three-electrode setup, rather than the two-electrode cell, which is usually the typical structure of practical electrochemistry devices, like fuel cells and electrolyzers.

The selection of reference electrode should ensure the accuracy of potential measurement. We recommend the use of reversible hydrogen electrode (RHE), which is commercially available. Alternatively, other reference electrodes can be used but the potential should be converted to RHE scale (performed by experimental calibration) to facilitate the comparison of results measured by various laboratories. Saturated calomel electrode (SCE) and Ag/AgCl, two of the most versatile reference electrodes in acid and neutral electrolyte, are based on the Cl-chemistry. However, their potential might not be stable in alkaline electrolyte, in which Hg/HgO is a more reliable choice.[22]

The gas inlet is necessary to make sure the measured current is purely contributed by ECSA, without the interference from the side reaction, i.e. ORR. The potential range for ECSA measurement usually overlaps with the range of ORR (<1.23 V vs. RHE). In this case, a trace amount of O_2 in electrolyte causes ORR, which interferes with ECSA measurement. To remove the dissolved O_2, before ECSA measurement, the electrolyte is purged with inert gas (e.g. Ar, N_2) through gas inlet to reach Ar- or N_2-saturation (usually takes 10~30 min; depends on the volume of electrolyte and gas flow rate); and during ECSA measurement, the electrolyte needs to be continuously bubbled with inert gas to maintain the Ar- or N_2-saturation.

The working electrode is the electrode where catalysts are located. Metal oxide catalysts can be made in powders (including nanoparticles) or thin films. Here we discuss the procedures of working electrode preparation for these two types of catalysts.

Powder catalysts are made into catalyst ink and drop-casted on a conductive substrate to form a homogeneous thin-film (as shown in Fig. 2b). To exemplify the detailed preparation procedures, we describe the protocols (as follows) modified from a landmark literature which aims to screen the ECSA of metal oxides by double layer capacitance method.[11] A glassy carbon disk (5 mm diameter) is used as the working electrode substrate. The disk is firstly polished by Al_2O_3 particle slurries with a diameter of 0.1 μm for 15 min, followed by polishing with 0.05 μm Al_2O_3 slurries for 15 min to give a mirror finish. Synthetic nap based polishing pad is used for polishing. After polishing, the disk is cleaned by sonicating sequentially in DI-water, acetone, and 2-propanol for 1 min each. The cleaned disk is then sonicated again in water for 1 min and it is now ready for use. The catalyst ink is made using 3.8 mL water, 1.0 mL 2-propanol, 40 μL of 5% Nafion 117 solution, and 80 mg of the oxide powder. Because this ink recipe aims to measure the ECSA via double layer capacitance, the powders for ink preparation contain only the native oxide and do not include conductive additives such as carbon black, which contributes to the capacitive current and interferes with ECSA measurement. This ink is sonicated for 30 min in ice bath, and then 10 μL of the ink is drop-casted onto mirror-polished glassy carbon disk using a micro-pipette. After drying in ambient condition, the as-prepared working electrode is ready for electrochemical measurement. We additionally remind the readers that with the purpose of measuring activity at metal oxide, carbon is usually added to ensure the conductivity; and the catalyst loading should be optimized by taking the loading mass that falls within the range where specific or mass activity remains constant as a function of loading mass.[22] We refer the readers to a recently published review[22] for the detailed working electrode preparation that aims at activity measurement.

Thin-film catalysts are intrinsically grown on the substrate by, for example, epitaxial growth,[23] electrochemical deposition,[1] spin-casting,[24] etc. To describe the protocols of working electrode preparation for thin-film catalysts, we give two exemplary models here. The first example is $La_{0.67}Sr_{0.33}MnO_3$ film epitaxially grown on Nb-doped $SrTiO_3$ (NSTO) substrate,[23] which is usually fabricated as a square sheet. The step-wise procedures are schematically shown in Fig. 2c. This film cannot be directly connected with potentiostat via the alligator clip of the cable, and thus the film is usually attached with a Ti wire, which serves as the conductive media. To affix the

electrical contacts between the Ti wire and the catalyst film, gallium−indium eutectic is scratched into the NSTO substrate, and the Ti wire is affixed with silver paint. The back and sides of the electrode, as well as the wire, are covered with a non-conductive, chemically resistant epoxy (e.g. Omegabond 101), only exposing the active region (the region that has catalysts) to electrolyte. We warn researchers that for thin-film catalysts, the epoxy covering is an especially crucial step to ensure that the non-active regions (regions that do not have catalysts) are not in contact with the electrolyte; otherwise, the non-active regions lead to capacitive current that not only interferes with the ECSA measurement, but also with the activity estimation. After epoxy covering, the working electrode is ready for ECSA measurement, and it is connected with the potentiostat by securing the alligator clip to the Ti wire. The second example is $Ni(Fe)O_xH_y$ films grown on Au substrate by spin-casting (see Fig. S1 for the schematic illustration of step-wise procedure).[1,24] Tinned-copper wire is attached to the substrate with silver paint, covered in epoxy, and attached to a glass tube with a liquid tight seal. After affixing the electrical contact, all tinned copper, silver paint, glass components, and epoxy are covered by hot glue (which is extruded from a heated glue gun) for impurity free analysis. After cooling down, the working electrode is ready for electrochemical measurement.

4. Techniques for determining the ECSA of metal electrocatalysts

The ECSA of metal electrocatalyst is usually measured by two types of methods: one is the coulombic charge of a specified surface faradaic reaction such as hydrogen underpotential deposition (HUPD), CO stripping, underpotential deposition (UPD) of metal and redox of surface metal; the other is the non-faradaic double layer capacitance (C_{dl}). This section only briefly introduces the mechanism of each method for ECSA measurement of metal, but does not detail the procedures. The detailed protocols are covered later in the next section for metal oxide.

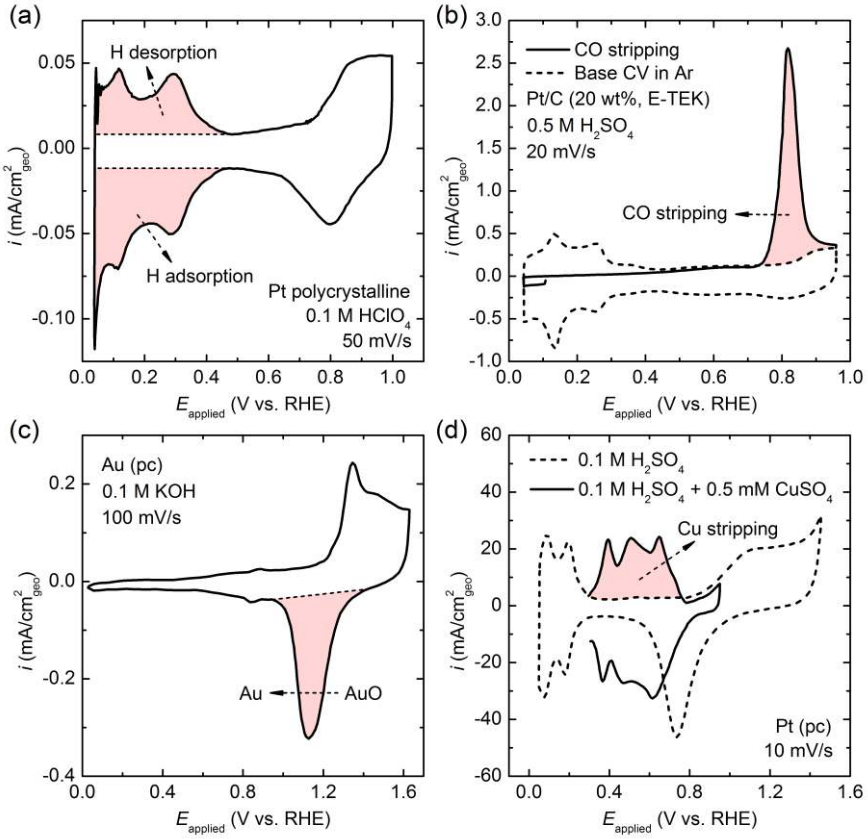

Fig. 3 (a) Hydrogen adsorption/desorption for measuring the surface area of polycrystalline Pt[4] at 50 mV/s in Ar-saturated 0.1 M $HClO_4$. Reproduced from ref. [4] with permission from American Chemical Society, copyright 2012. (b) CO stripping that quantifies the surface area of Pt/C[5] at 20 mV/s in Ar-saturated 0.5 M H_2SO_4. Reproduced from ref. [5] with permission from The Electrochemical Society, copyright 1998. (c) Surface redox for the surface area of Au (pc),[7] namely polycrystalline Au. Reproduced from ref. [7] with permission from Royal Society of Chemistry, copyright 2013. (d) Underpotential deposition of Cu for measuring the surface area of Pt (pc),[6] namely polycrystalline Pt. Reproduced from ref. [6] with permission from American Chemical Society, copyright 2012.

The HUPD is based on the adsorption and desorption of H atoms (which usually originate from a protic solvent, e.g., water) at metal surface. For example, the cathodic formation of an H monolayer at Pt and its anodic desorption are represented by the CV peaks ranging from ~0.05 to ~0.4 V vs. RHE (Fig. 3a). The H desorption and adsorption region are integrated after subtracting the double-layer currents. The resulting coulombic charges under the shaded regions in Figure 2a are averaged, and divided by the specific charge (210 $\mu C/cm^2_{Pt}$ for a monolayer HUPD at Pt)[7] to give the ECSA of Pt. The HUPD has been widely used for determining the

ECSA of some noble metals such as Pt,[7,25] Rh[25] and Ir,[25] and particularly Pt-based alloys[26] for various electrocatalytic studies.

The CO stripping quantifies the surface area via recording the charge transfer of stripping one monolayer of CO at metal surface. With CO stripping at Pt[5] as the example, the adsorption of a CO monolayer at Pt is triggered by bubbling CO gas into the electrolyte while applying a mild reducing potential, i.e. 0.1 V vs. RHE, on working electrode. Prior to the stripping CV measurement, the electrolyte is purged with Ar gas to remove the dissolved CO gas, and at the same time, the working electrode is held at 0.1 V vs. RHE. The stripping of CO is signified by the oxidation peak at ~0.7 V vs. RHE (shaded area in Fig. 3b), and the peak is integrated with a baseline determined by CV recorded in Ar-saturation under the same scan rate (i.e. 20 mV/s). To convert the charge of CO stripping to the surface area of metal, a specific charge of 420 $\mu C/cm^2_{Pt}$ (for the formation of a CO monolayer at Pt) is used. In analogous to H adsorption method, CO stripping is commonly used for Pt-based catalysts,[26] as well as Rh[25] and Ir.[25]

For the metals, which do not possess the characteristic CV peak of H deposition or CO stripping, the surface area can be alternatively quantified by the redox reaction of surface metal, which relies on the interaction between the surface metal atoms and oxygenated species. The CV peak that refers to the anodic formation of one monolayer of metal oxides or its reduction is integrated and converted to the surface area via a specific charge. The well-published examples are given as follows:[7] the reduction peak of $Ni(OH)_2$ (~0.05 V vs. RHE) depicts the surface area of Ni with a specific charge of 514 $\mu C/cm^2_{Ni}$; 400 $\mu C/cm^2_{Ag}$ is used to convert the formation of one monolayer of AgOH or Ag_2O (~1.25 V vs. RHE) to the surface area of Ag; at Cu, 360 $\mu C/cm^2_{Cu}$ corresponds to the formation of one monolayer of Cu_2O (the broad anodic peak between 0.5 V and 0.7 V vs. RHE); the reduction peak of AuO centered at ~1.1 V vs. RHE (the shaded area in Fig. 3c) with 390 $\mu C/cm^2_{Au}$ for Au surface area; the oxide reduction peak located at ~0.75 V corresponds to a charge density of 424 $\mu C/cm^2_{Pd}$ for Pd.

In analogous to CO stripping (which utilizes CO as the probe molecule), underpotential deposition (UPD) uses the metal ions from the electrolyte as the probe. To exemplify this method, we illustrate the determination of polycrystalline Pt surface area with Cu as the probe atom (Fig. 3d).[6] In the mixture of H_2SO_4 and $CuSO_4$, the monolayer of Cu is electrochemically deposited by holding Pt at the deposition potential for a required duration (for example, 0.3 V vs. RHE for 100 s). Immediately after the deposition, an anodic scan is performed starting from the deposition potential (i.e. 0.3 V vs. RHE) to the region (e.g., 1.0 V vs. RHE) where Cu_{upd} is thoroughly stripped off. The anodic peaks for Cu_{upd} stripping are integrated with the baseline determined by CV of polycrystalline Pt in the absence of $CuSO_4$. Based on a specific charge of 420 $\mu C/cm^2_{Cu}$, the coulombic charge of Cu_{upd} stripping is converted to the surface area of polycrystalline Pt. UPD has been widely used to measure the surface area of noble metals such as Pt, Au, Ag and Ru with the probe atoms such as Cu, Ag, Pb, Hg.[6,10]

The double layer capacitance (C_{dl}) is a quantitative indicator of the surface area that is accessible to the electrolyte ions. For example, to measure the surface area of Co, the CV in 0.1 M KOH under various scan rates is collected at 0.87 V ~ 0.97 V vs. RHE,[7] which is the potential window of double layer region without interference from the faradaic charge transfer. The current density at the middle potential (0.92 V vs. RHE) is linearly dependent on the scan rate. Its slope is divided by a specific capacitance of 60 $\mu F/cm^2_{Co}$ to give the surface area of Co.[7] Since almost all metal materials have the feature of C_{dl} under CV scans, this method is, in principle, considered as a universal way to extract the surface area of all metal catalysts. However, the limitation is the specific capacitance, which possibly varies, depending upon the electrode potential, surface structure, electrolyte composition/concentration; even the same metal fails to reach a general agreement on the value of the specific capacitance.[9,22]

5. Techniques for determining the surface area of metal oxide electrocatalysts

On the basis of those ECSA techniques for metals, their principles and methodologies can be implemented to the ECSA measurement of metal oxides. For each method (including ECSA and non-electrochemistry method), we describe the detailed procedures for guiding the experiment, and discuss the rationales and uncertainties to remind readers of the applicability.

5.1 Surface redox reaction

The surface redox reaction at metal oxide tells the number of active atoms, but it is still challenging to convert the CV peak to ECSA. In this section, we start from rationalizing that the surface redox reaction at metal oxide can quantify the number of active atoms and giving a few relevant exemplary applications. Then with a literature example, we describe the ECSA estimation by surface redox reaction, followed by discussing the major difficulties in this methodology.

The CV peak denoting oxidation/reduction of metal oxide is expected to quantify the ECSA, because the coulombic charge under CV peak is quantitatively associated with the number of electrochemically accessible surface atoms. Some examples of using CV peak to quantify the redox active atoms can be found in a series of Ni-Fe-Al spinel oxides,[27] where the Ni^{2+}/Ni^{3+} reduction peak has been integrated to quantify the redox active Ni cations; $Ni_{0.8}Fe_{0.2}O_xH_y$ film,[1] where the oxidation peak of Ni^{2+}/Ni^{3+} measures the number of redox active Ni (Fig. 4a); and the cathodic peak reflecting the reduction of Mn cations from its original valence state (determined by X-ray photoelectron spectroscopy) to Mn^{2+} extrapolates the number of active Mn in a series of $Mn_xFe_{3-x}O_4$ spinel oxides.[28] Thus, in principle, the ECSA can be obtained from the coulombic charge under the CV peak of metal oxide oxidation/reduction with a known specific charge. Different from the metal catalyst, where CV peak for ECSA measurement has been widely used and the reliability has been well demonstrated, however, the application of metal oxide CV peaks for ECSA quantification is merely reported and the approach at present is still questionable.

To explain its limitations/problems, we scrutinize an exemplary application of surface redox reaction in ECSA determination of electrochemical-deposited nano-structured Mn (III) oxide OER catalyst.[29] The procedures are described as follows.[29] The CV is recorded in N_2-saturated 0.1 M KOH, and the charge of the

oxidation peak at ~0.9 V vs. RHE (which is assigned to the transition from Mn^{3+} to Mn^{4+}) is integrated. To convert the integrated charge to surface area, the specific charge is obtained by simplified calculation. The denominator of specific charge ($\mu C/cm^2_{oxide}$), which is area (cm^2_{oxide}), is estimated based on the crystal lattice of α-Mn_2O_3; and its numerator, which is coulomb (μC), is calculated by assuming that the oxidation reaction penetrates only one α-Mn_2O_3 monolayer, where each Mn cation losses one electron.

As demonstrated by the above example, the challenges of utilizing CV peak for measuring the ECSA of metal oxide mainly stems from the following four obstacles. First, it is not understood whether the CV peak of metal cations is associated with the redox reaction within one monolayer or multilayers, which affects the estimation of specific charge. As proposed by this study, the oxidation is likely to penetrate deeper than one monolayer.[29] This unknown reaction depth at metal oxide is different from the metal catalyst, where the specific charge is well-defined because the corresponding CV peak relates to the redox reaction of one monolayer, for example, the formation of one Cu_2O monolayer for Cu ECSA,[7] one monolayer of AgOH or Ag_2O for Ag.[7] Second, the specific charge of the same metal oxide might vary with synthesis method, surface orientation, etc. For example, with the aid of atomic force microscopy (AFM), the specific pseudocapacitive charge (including double layer capacitance) on rutile IrO_2(100) and RuO_2(100) are determined as 130 and 140 $\mu C/cm^2_{oxide}$, respectively, which are higher than that of (110) surface: 90 $\mu C/cm^2_{oxide}$ for IrO_2 and 100 $\mu C/cm^2_{oxide}$ for RuO_2.[19] Considering this discrepancy, either the calculated specific charge (which is based on a simplified model) or the experimental measured value on a particular material might not be universally applicable. Third, the number of electrons transferred per metal site is usually determined by assumption, which possibly deviates from the true situation. For example, the characteristic oxidation peak of Ni^{2+}/Ni^{3+} is used for quantifying the

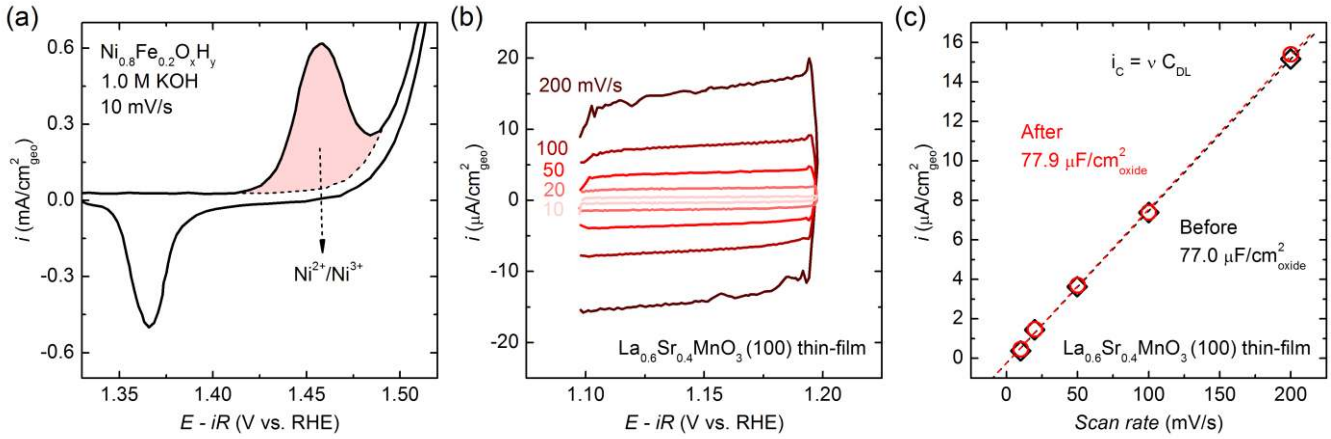

Fig. 4 (a) An exemplary CV of $Ni_{0.8}Fe_{0.2}O_xH_y$ film[1] shows the integration of the first anodic peak for quantifying the redox active Ni. The OER is subtracted by an exponential baseline. Reproduced from ref. [1] with permission from American Chemical Society, copyright 2017. (b) (c) The demonstration of determining the surface area by double-layer capacitance (C_{DL}) method.[30] (b) CVs of (100)-oriented $La_{0.6}Sr_{0.4}MnO_3$ film[30] (20 nm) in Ar-saturated 0.1 M KOH at various scan rates show the rectangular shape. The CVs were smoothed by a second-order polynomial filter in EC Lab (seven point window). (c) The specific capacitance of a (100)-oriented $La_{0.6}Sr_{0.4}MnO_3$ film (20 nm) extracted from C_{DL} measurements using the EEL setup before (diamonds) and after storage in air for a week followed by OER measurements (circles). The specific C_{DL} capacitance was normalized by the geometric disk area and the roughness factor obtained from AFM. (b and c) are reproduced from ref. [30] with permission from American Chemical Society, copyright 2016.

redox active Ni with the assumption that it is a one electron transfer redox (Fig. 4a).[1,31] This 1 e^- assumption has been confirmed to be correct at $Ni_{0.8}Fe_{0.2}O_xH_y$ films.[1,31] However, others have revealed that the redox may involve Ni in oxidation states other than 3+, and calculated up to ~1.67 e^- per Ni site.[31] This issue thus requires accurate estimation of initial and final oxidation state of the metal cations. Fourth, integrating the CV peak could be difficult to unambiguously extract the coulombic charge for the redox of metal cations. The uncertainty comes from the determination of a baseline, which aims to subtract the background current. In CO stripping or UPD at metal catalysts, the baseline is accurately determined by a separate measurement (for example, a baseline determined by CV recorded in Ar-saturation for CO stripping method; a baseline determined by CV in the absence of $CuSO_4$ for UPD method). However, the baseline for CV peaks of metal oxide oxidation/reduction is drawn manually. The determination of baseline can be further exacerbated by the fact that the characteristic CV peak of some metal oxides such as Ni-containing oxyhydroxide[1] (for example, as shown in Fig. 4a) overlaps with the OER onset current.

Up to date, despite these challenges and the poor development, the surface redox is highly expected to have the capability of quantifying the surface area of metal oxide, because this method is based on CV peak, which is in essence a powerful surface-sensitive technique. Systematic studies that correlate the CV peaks with metal oxide surface area are strongly encouraged in the near future.

5.2 Double layer capacitance

Due to the lack of knowledge on the surface redox reaction at metal oxides, double layer capacitance (C_{DL}) is currently the most popular method for measuring ECSA of metal oxides. We discuss

the protocols for measuring the ECSA by C_{DL}, and analyze the uncertainties of this method.

With the epitaxially grown (100)-oriented $La_{0.6}Sr_{0.4}MnO_3$ thin-film[30] as an example, we describe the procedures of CV-derived C_{DL} measurement. In Ar-saturated 0.1 M KOH, the CVs under various scan rates (10, 20, 50, 100, and 200 mV/s) are recorded within 1.1 ~ 1.2 V vs. RHE (Fig. 4b), where there is no faradaic current response. At the middle of the potential window,[30] the double layer capacitive current (i_C) is taken as either the anodic or cathodic current or the average of the anodic and cathodic current. The i_C is plotted against the scan rate v, and i_C follows the expected linear behavior of an ideal capacitor with scan rate v, given by $i_C = v\ C_{DL}$. The slope of this straight line is C_{DL}, which is converted to ECSA via a specific capacitance of 77 $\mu F/cm^2_{oxide}$ (determined by AFM). Another technique for measuring the C_{DL} is electrochemical impedance spectroscopy (EIS),[32] which is less frequently used than CV. The EIS measurement applies a sinusoidal potential that is performed within the same non-faradaic region as CV. The frequency-dependent complex impedance is recorded and fitted by the modified Randles circuit to generate the C_{DL}. It has been reported that C_{DL} measured by EIS and scan rate-dependent CV agree well within ±15%.[32] Note that in electrocatalysis tests, the conductive additive such as carbon black is usually indispensable to drop-casted electrode for ensuring smooth charge transfer at catalyst interface and maximizing the utilization of oxide surface.[33] Without the conductivity provided by carbon, pure metal oxide powders give quite substandard performance,[33,34] and it is thus hard to define the intrinsic activity. However, for the purpose of getting the C_{DL} purely contributed by oxides, the electrode prepared by drop-casting method does not include carbon, because the high-surface-area carbon contributes to the non-faradaic current and interferes with the ECSA estimation.

The same as the studies on metal catalysts, the uncertainty of the metal oxide ECSA estimated by this C_{DL} method also originates from the determination of the specific capacitance. At the current stage, the specific capacitance of metal oxide is usually unknown, and thus this parameter is mostly determined by directly referencing a popular value from the literature. However, as mentioned in the previous section, it is highly possible that the specific capacitance varies, depending upon the electrode potential, surface structure, electrolyte composition/concentration; even the same metal oxide cannot reach a general agreement on the value of the specific capacitance. For example, with the aid of AFM, the specific capacitance of (100)-orientated $La_{0.6}Sr_{0.4}MnO_3$ thin-film epitaxially grown on conductive substrate is proved to be 77 $\mu F/cm^2_{oxide}$.[30] This is larger than 40 $\mu F/cm^2_{oxide}$,[35] which is considered as a universal specific capacitance for metal oxide surfaces. Some studies consider 60 $\mu F/cm^2_{oxide}$ is universal.[8] Moreover, the specific capacitance of $Ni(Fe)O_xH_y$ thin-film is determined to be ~80 uF/cm^2_{oxide},[1] which is also larger than the average value suggested for oxide systems. With the aid of AFM, a recent study further proves that the universal value of specific capacitance is not reliable, as oxide surfaces differ a lot (as shown in Fig. 5).[36] Considering this discrepancy between the universal value and real situation, we remind readers to remain attentive to the resulting accuracy of C_{DL}-based ECSA.

The C_{DL} measurement can be convoluted by the fact that the measured i_C is usually not purely contributed by double layer current; the measured i_C might result from some side reactions at the interface such as corrosion, intercalation, and specific adsorption.[36] These side reactions are particularly pronounced at metal oxides surfaces, where H^+/OH^- adsorption generates additional currents.[36] As a result, the specific capacitance is largely overestimated, which can be demonstrated by a few examples shown in Fig. 5. The C_{DL} of 19 materials are screened in 0.15 M $NaClO_4$ and normalized to the surface area determined by AFM to

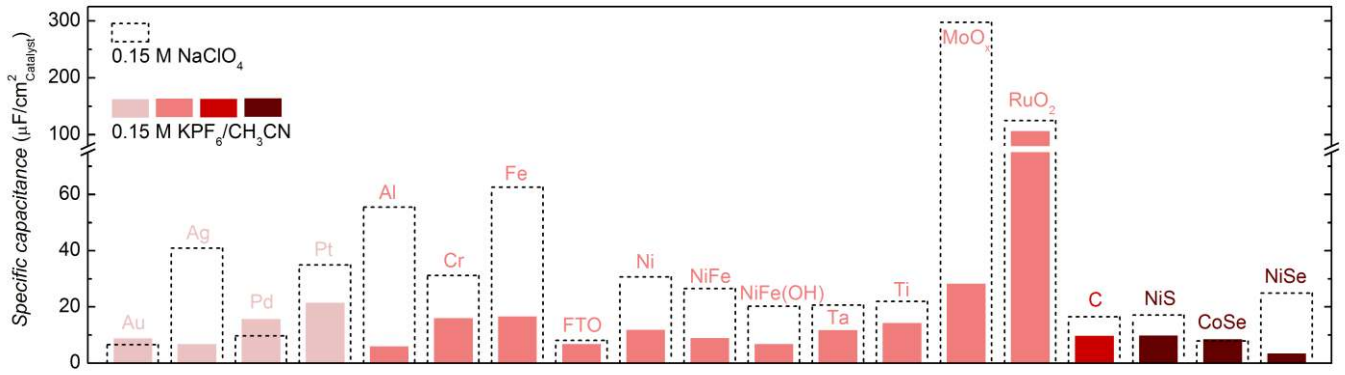

Fig. 5 Comparison of specific C_{DL} (double layer capacitance) values of 4 classes of materials measured in aqueous electrolyte (0.15 M $NaClO_4$) and aprotic electrolyte (KPF_6/CH_3CN). These 4 sets of materials are presented in various colours (from left to right): noble metals (Au, Ag, Pd, Pt), surface oxide passivated base metals (Al, Cr, Fe, FTO (fluorine-doped tin oxide), Ni, NiFe, NiFe(OH), Ta, Ti, MoO_x, RuO_2), carbon (C), and metal chalcogenides (NiS, CoSe, NiSe).[36] All the C_{DL} measurements were performed by recording cyclic voltammetry (CV) over a narrow range (±50 mV) centered at the open circuit potential (OCP). The CV scan rates range from 5 to 50 mV/s. Reproduced from ref. [36] with permission from American Chemical Society, copyright 2018.

generate the specific capacitances.[36] Noble metals (such as Au and Pd) have specific capacitances of ~8 $\mu F/cm^2_{metal}$, which is at the low end of the values typically assumed for a metal surface.[36] In contrast, despite the use of $NaClO_4$ electrolyte has minimized the interference from specific adsorption of electrolyte ions, materials with oxide surface exhibit specific capacitances of 2~6 times larger

than that of these noble metals. This phenomenon has been well documented and this enhancement is attributed partially to H^+/OH^- adsorption at oxide surface.[36] As evidenced, we remind the readers that due to the side reactions during C_{DL} measurement, not only the specific capacitances are overestimated, but also these values shows a wide variability across various materials, which leads to the uncertainty of the C_{DL}-derived ECSA. To avoid/minimize the interference from the side reactions, the accuracy of C_{DL} measurement is significantly improved in polar aprotic electrolyte (KPF_6/CH_3CN, as shown in Fig. 5),[36] where the specific capacitances are generally smaller and obviously have a less variability than those measured in aqueous electrolyte. This aprotic electrolyte method is a simple and powerful tool for estimating the C_{DL}-based ECSA. However, the imperfection presents: known supercapacitor materials such as RuO_2 and oxide-passivated Mo (MoO_x) still display significant ion transfer currents,[36] indicating the universality of C_{DL} measurement in polar aprotic electrolyte is still a challenge.

Except of the uncertainty about the specific capacitance and convoluting side reactions, the electrical conductivity of metal oxide also affects the measurement of its surface area by the C_{DL} method. To prove this point, with 16 metal oxides (in the forms of powders) as the model materials, the ECSA estimated by C_{DL} are screened and compared with the surface areas measured by Brunauer-Emmett-Teller (BET),[11] which is a universal method that accurately characterizes surface area. It is observed that (Fig. 6a), the C_{DL}-based ECSA of metallic-like oxide with high conductivity, such as IrO_2, RuO_2, $LaNiO_3$ and $LaCoO_3$, is consistent with its BET surface area. In contrast, such consistency between the surface areas extracted by these two methods is not observed at semiconducting and insulating metal oxides with low conductivity, such as NiO, Co_3O_4, $NiCo_2O_4$, and CoO, which show much lower C_{DL}-based ECSA than BET surface area. Interestingly, most of these low-conductivity oxides give similar C_{DL}-based ECSA (~ 1 m^2/g), regardless of the BET surface area. This finding indicates that the C_{DL} is capable of reflecting the real surface area of conductive metal oxides, but not applicable to the metal oxides with low conductivity, which is postulated to be caused by the dielectric behavior of the semiconductors or insulators.[11] The effect of electrical conductivity on estimated C_{DL} is also reported in $Ni(Fe)O_xH_y$ thin film,[1] where the C_{DL} measured by EIS is correlated with the potential-dependent conductivity of the thin film. At the potential region of low conductivity, the C_{DL} is quite low (nearly 0 mF/cm^2_{geo}, normalized to the geometric area of electrode), simply the capacitance of the underlying flat substrate, and keeps unchanged with increasing mass loading of $Ni(Fe)O_xH_y$. In contrast, at the potential region of high conductivity, the C_{DL} is up to 3 orders of magnitude larger the low conductivity region and scales linearly with mass loading of $Ni(Fe)O_xH_y$. These above evidences indicate that C_{DL} measurements are only a reliable indicator of ECSA when the catalyst has high electrical conductivity.

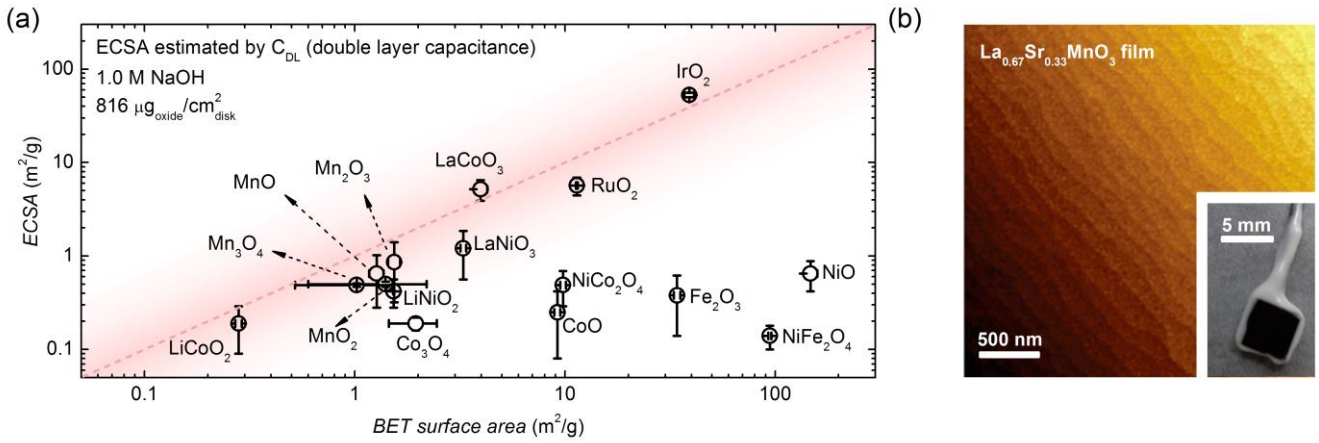

Fig. 6 (a) The comparison between the C_{DL}-estimated electrochemical active surface area (ECSA) of 16 metal oxides powders (assuming a specific capacitance of 40 $\mu F/cm^2_{oxide}$) and the surface areas measured by Brunauer-Emmett-Teller (BET).[11] The electrodes are prepared without adding carbon. Reproduced from ref. [11] with permission from Royal Society of Chemistry, copyright 2016. (b) The demonstration of determining the surface area of thin film catalysts by atomic force microscopy (AFM). An exemplary AFM image of $La_{0.67}Sr_{0.33}MnO_3$ films,[23] with a vertical contrast scale of 7.8 nm. Inset is the exemplary photograph of an epitaxial thin-film electrode (5 × 5 mm^2). Reproduced from ref. [23] with permission from American Chemical Society, copyright 2015.

5.3 Atomic force microscopy

Due to the lack of knowledge about the ECSA measurement of metal oxide, the determination of catalyst surface area currently has to rely on non-electrochemistry techniques. Atomic force microscopy (AFM) is capable of reliably evaluating the surface area of metal oxide with high accuracy, but it is only applicable to the thin-film electrodes (such as epitaxially grown and electrodeposited thin-film electrodes) with well-defined surface and low roughness. Exemplary applications can be found in $La_{1-x}Sr_xMnO_3$,[23,30] IrO_2,[19] RuO_2,[19,36] $SrIrO_3$,[37] $IrO_x/SrIrO_3$,[38] $Ni(Fe)O_xH_y$,[1] etc. Here, with the epitaxially grown $La_{0.6}Sr_{0.4}MnO_3$ thin-film[23] as an example, we describe the procedures of measuring surface area by AFM. As mentioned earlier, the working electrode of $La_{0.6}Sr_{0.4}MnO_3$ thin-film is fabricated as a square sheet attached with a conductive wire, i.e. Ti wire (Fig. 6b, inset). The back and sides of the electrode, as well as the wire, are covered by non-conductive and chemically stable polymer materials such as epoxy, only exposing the catalyst surface to electrolyte (Fig. 6b, inset). Then the geometric surface area that

is accessible to the electrolyte is quantified by optic microscopy, and converted to the surface area of catalyst via the roughness factor determined by AFM (Fig. 6b). The accuracy of specific activity estimated with thin-film electrode is considered to be the highest, not only because the influences of conductive additives (such as carbon) and Nafion binders are ruled out, but also the uncertainty in the measurement of surface area is excluded by the employment of AFM.[39]

5.4 BET

Due to the difficulties in determining the ECSA (as discussed above), BET surface area is at present the best alternative way for extracting the specific activity of powder metal oxide catalysts. BET takes advantage of the isothermal physical adsorption of probe gas molecules (most frequently N_2, in some cases, CO, O_2, H_2, etc.) on a solid surface to measure the specific surface area of materials. Although it is unambiguously believed that BET accurately measures the surface area of powder materials, the major concern is the validity of using BET surface area for the extraction of specific activity. The BET surface area is definitely not equivalent to the real ECSA, but it is a reasonable reflection of real ECSA. For example, the validity can be demonstrated by examining the relationship between the coulombic charges under the characteristic CV peak of Co_3O_4 spinel oxides with various particle sizes and their BET surface areas. As shown in Fig. 7a, since the area under CV peak describes ECSA, the smaller sized Co_3O_4 gives a larger redox peak of Co^{3+}/Co^{4+} (~1.45 V vs. RHE). By integrating the cathodic peak (Fig. 7b, inset), the coulombic charge scales linearly with BET surface area (Fig. 7b), indicating that BET is capable of being a reasonable representative of ECSA on the ink-casted electrode for powders. Such observation can also be found in a series of Ni-Fe-Al spinel oxides,[27] where BET trends well with the number of redox active Ni, as determined by CV integration. The reliability of BET surface area for specific activity determination is further proved by the observation that the specific OER/ORR activity of oxide particles (electrode prepared by ink drop-casting) estimated by BET method agrees well with the activity

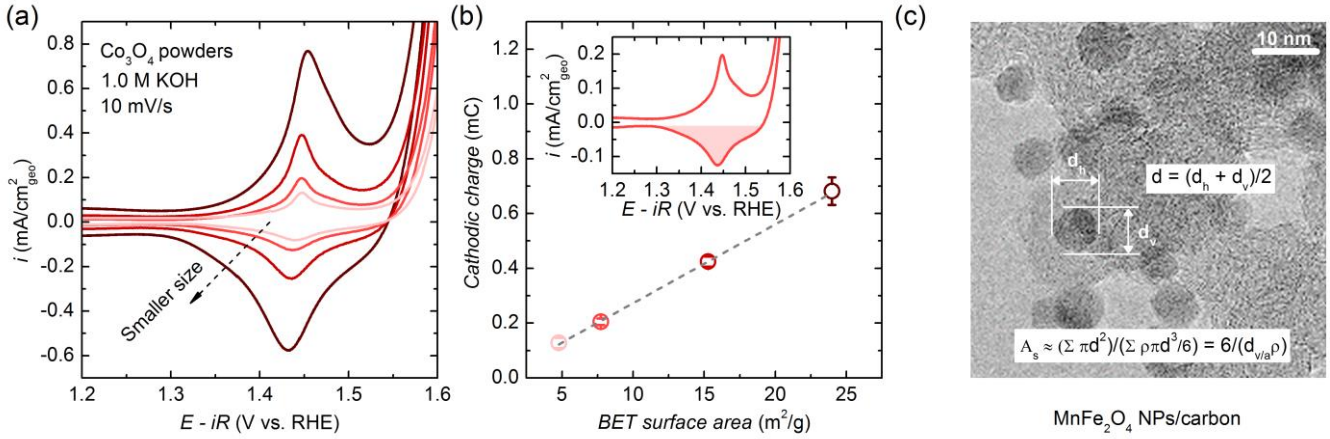

Fig. 7 (a and b) The correlation between the coulombic charge (Q) of surface redox reaction and Brunauer-Emmett-Teller (BET) surface area, which is exemplified by Co_3O_4 spinel oxides[40] with various particles sizes. (a) CV of Co_3O_4 (b) Q of cathodic Co^{3+}/Co^{4+} peak at various Co_3O_4 as a function of BET surface area. Inset is an exemplary integration of cathodic Co^{3+}/Co^{4+} peak. (a and b) are reproduced from ref. [40] with permission from Elsevier, copyright 2018. (c) Determining the surface area (A_s) of $MnFe_2O_4$ nanoparticles (NPs)[41] by transmission electron microscopy (TEM) image, where the measurement of particle size and calculation of A_s is shown. The NPs are loaded on Vulcan carbon. Reproduced from ref. [41] with permission from Springer Nature, copyright 2017.

measured at well-defined epitaxial oxide thin-film surfaces (of comparable oxide chemistry),[2,39] which is considered as a highly accurate method for estimating specific activity. The specific activity extracted by BET surface area has been widely used and has guided the discovery of landmark ORR/OER activity descriptors such as e_g,[20,21,42,43] the covalency of metal-oxygen bond,[20,21,44] the position of O-2p band center[45,46] and the charge transfer energy.[47] We recommend that, to validate the employment of BET surface area in electrochemical practices, especially for screening catalysts of various particle sizes, researchers should verify that the BET surface area is in accordance with the C_{DL} or a particular CV peak. For example, the BET surface areas of $LaCoO_3$ with various particle sizes trend well with their double layer capacitances,[43] and the same observation is reported at $MnCo_2O_{4+\delta}$ particles with different sizes,[42] demonstrating that the difference of particle sizes characterized by BET is reflected on the drop-casted electrode.

5.5 Electron microscopy

To exemplify the procedures for measuring the surface area by electron microscopy, we present an example that estimates the surface area of $MnFe_2O_4$ NPs[41] which are loaded on Vulcan carbon. By the transmission electron microscopy (TEM) imaging (Fig. 7c), the diameter (d) of each $MnFe_2O_4$ particle is obtained by averaging the distance along the horizontal direction (d_h) and that at vertical (d_v). To improve the reliability of the statistical analysis result, we recommend researchers to perform the above measurement at a large number of particles (at least 200 particles). In this case of $MnFe_2O_4$ NPs/carbon, by measuring and averaging d of at least 200 particles, the $d_{v/a}$ is obtained (see the histogram of diameter in Fig. S2 for $d_{v/a}$ estimation). By assuming a spherical geometry approximation,[20,21,48] the surface area is calculated according to equation as shown in Fig. 7c, where A_s is the specific surface area, ρ is the oxide bulk density (i.e. 5.368 g/cm^3 for $MnFe_2O_4$).

The error of this electron micrograph-based surface area mainly originates from the discrepancy between the assumption that all particles are spherical and the real morphology, which is usually irregular. Moreover, the material density (ρ) is usually unknown and taken as the bulk density, which might affect the accuracy. As a result of the spherical approximation and density uncertainty, the surface area estimated by TEM or scanning electron microscopy (SEM) observation is considered to be less accurate than other techniques. However, the accuracy of this electron microscopy method has been reported to be reasonably reliable, as evidenced by the finding that surface areas of oxide catalyst ($LaNiO_3$ and $Ba_{0.5}Sr_{0.5}Co_{0.8}Fe_{0.2}O_{3-\delta}$) determined by SEM and BET measurement agree well within a factor of 2-3.[20,21] Similar evidence is also found in the case of Pt NPs, where the surface area estimated by TEM and ECSA measured by H adsorption/desorption are within a factor of 2~3.[49] Therefore, despite the uncertainty resulting from the spherical assumption, the electron microscopy acts as a promising alternative method that is particularly applicable to the following two sets of powder catalysts. First, this method is recommended for powders which do not have sufficient weight for BET measurement, especially the nanostructured metal oxides that are synthesized with very limited yield. Second, for metal oxide-based composites where the electrocatalytic-active metal oxide particles are dispersed or grown on the inactive supporting materials such as carbon, it is hard to separate the surface area of metal oxide (which is usually considered as the active component) from that of the composite by BET or C_{DL} measurement. Since TEM provides the contrast difference of these two materials, the surface area of metal oxide is extractable.

Table 1. A summary and comparison of experimental techniques for measuring the surface area of metal oxide electrocatalysts.

Method	Catalyst	Accuracy	Weakness(es)
Surface redox reaction	Powder, thin-film	Low	1. Not sure if the CV peak relates to one-monolayer-reaction or multilayers; 2. A lack of well-accepted tabulated specific charge, which might vary with synthesis method, surface orientation, etc.; 3. The number of electron transferred per metal site is not known; 4. The difficulty in determining the baseline for integration of CV peak.
Double layer capacitance (C_{DL})	Powder, thin-film	Medium-high	1. A lack of well-accepted tabulated specific C_{DL}, which might vary with the electrode potential, surface structure, electrolyte composition/concentration, etc.; 2. The C_{DL} measurement can be convoluted by some side reactions, e.g. corrosion, intercalation, and specific adsorption; 3. Only reliable in the case that the metal oxide has high electrical conductivity.
Atomic force microscopy (AFM)	Thin-film	High	Only applicable to thin-film catalysts with low roughness factor.
Brunauer-Emmett-Teller (BET)	Powder	Medium-high	1. BET surface area is not equivalent to the "real" ECSA; 2. The weight of catalysts needs to be sufficiently large for sound BET analysis.
Electron microscopy	Powder	Medium	1. The discrepancy between the assumption that all particles are spherical and the real morphology, which is usually irregular; 2. The material density is assumed to be the bulk oxide density.

6. Recommendations on technique selection

After discussing the procedures, rationales and limitations of the above five techniques for measuring the surface area of metal oxide catalysts in Section 5, this section presents our recommendations on selecting a reasonable technique for a particular metal oxide electrocatalyst; and reminds the readers that, at present, there is unfortunately no perfect method for surface area estimation.

We briefly list the applicability and weaknesses of each method in Table 1, which instructs the selection of technique for surface area measurement of metal oxide catalysts. For all metal oxide electrocatalysts (either powder or thin-film), we recommend the ECSA method (surface redox reaction or C_{DL}) as the top choice if the weaknesses shown in Table 1 can be overcome; otherwise, we recommend the non-electrochemistry method. In the case of thin-film catalyst, we recommend researchers to extract the specific activity based on AFM-derived surface area. In the case of powder catalysts, BET is preferred. If the amount of powder catalysts is not enough for BET measurement, we recommend the electron microscopy method for estimating the surface area. In the case that the powder catalysts are composites, such as metal oxide particles grown on carbon, we recommend the readers to obtain the surface area by measuring the size of the metal oxide particles in TEM images.

We wish to remind the researchers that, as indicated by the weakness(es) in Table 1 (and evidences presented in Section 5), either these ECSA methods or non-electrochemistry methods are not, by all means, perfect for surface area measurement. It should be noticed that it is actually quite challenging to estimate the "real" ECSA. The surface area estimated by electrochemistry method is not necessarily the "real" ECSA, because the ECSA measurement usually does not probe the interaction between the electrocatalytic sites and the reaction intermediates. For example, the C_{DL}-based

ECSA is the surface area that is accessible to electrolyte ions; the CV peaks denote the interaction with oxygenated species, but the sites that are available for self-oxidation/reduction do not equal the "real" active sites for catalysis. Although there is no perfect method, the convenient ECSA measurements and non-electrochemistry methods still enable these surface-sensitive

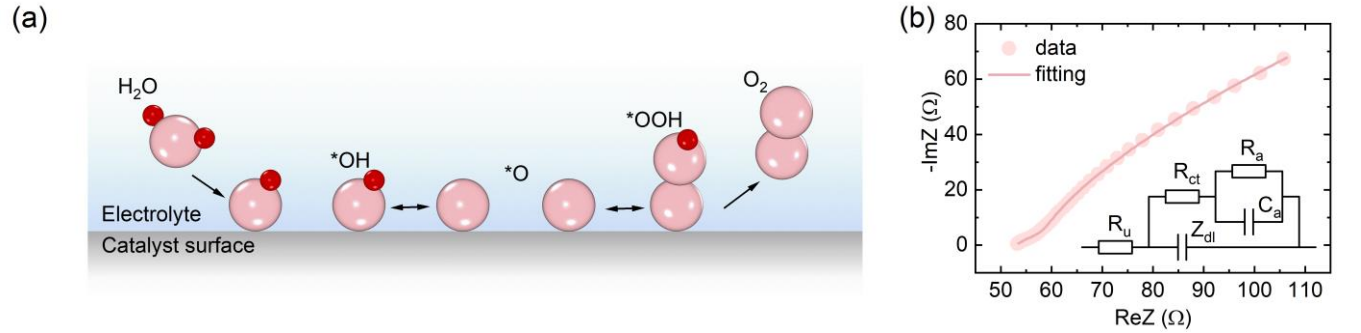

Fig. 8 (a) The schematic illustration that explains the origin of the adsorption capacitance (C_a) of oxygen evolution reaction (OER) intermediates for surface area measurement. *OH, *O and *OOH denote OER intermediates where the redox transformations between them can be quasi-reversible with reproducible relevant physico-chemical parameters at a given electrode potential. As these transformations are surface limited, the adsorption capacitance is a parameter which is very sensitive to the electrochemical active surface area (ECSA) of the oxide electrodes. (b) An exemplary impedance Nyquist plot of the NiO_x thin-film electrode in 0.1 M KOH at 1.6 V vs. RHE. Open square is the measured data; the line is fitting result to the model as shown in the inset. The equivalent electric circuit used to analyze the impedance data includes uncompensated resistance (R_u), the charge-transfer resistance (R_{ct}), the impedance of the double layer (Z_{dl}), the adsorption resistance (R_a), and capacitance (C_a) to describe the contribution of the reversibly adsorbed reaction intermediates to the impedance response. (a and b) are reproduced from ref. [50] with permission from John Wiley and Sons, copyright 2016.

techniques to act as valuable tools for screening specific activity and revealing the electrocatalysis mechanisms.

7. Perspective

The present-day lack of ECSA knowledge at metal oxides calls for improved accuracy of current ECSA techniques. In particular, systematic studies on the quantitative correlation between surface redox reaction and ECSA, more abundant database of specific capacitances for C_{DL}-based ECSA are needed. To avoid the weaknesses of the techniques discussed in Section 6, developing novel and more reliable techniques for surface area determination is also necessary. Here we provide an example of a new EIS technique, which measures ECSA via the adsorption capacitance (C_a) of the adsorbed oxygenated species during OER.[50]

Similar to the adsorption of hydrogen atoms or CO molecules in the case of metal electrodes, the mechanism of this C_a method uses oxygenated intermediates during OER as probe for ECSA estimation. The adsorption capacitance is directly proportional to the average (in time) number of the intermediates located exactly at the surface and its physical meaning is expressed as $C_a = -q_a(d\theta_a/dE)$, where θ_a is the effective adsorbate fractional coverage oscillating during the impedance probing at a given electrode potential, q_a is the charge to form a saturated layer of the adsorbed species. Fig. 8a schematically illustrates the origin of the adsorption capacitance related to the OER intermediates and explains predominant localization of these adsorbates at the metal oxide surface.

With NiO_x thin film electrodeposited at a polycrystalline Pt electrode (diameter = 5 mm), the procedures for C_a-derived ECSA are described as follows.[50] Immediately after the film formation, CV is cycled between 0.93 and 1.73 V vs. RHE at the scan rate of 50 mV/s in Ar-saturated 0.1 M KOH. After the 3rd cycle, a slower scan rate of 1 mV/s is set between 1.43 V and 1.53 V vs. RHE. The EIS measurements are then conducted in a staircase mode with the interval of 0.01 V from 1.53 V to 1.63 V vs. RHE. For the EIS experiments, a shunt capacitor of ~4 μF was connected between reference and counter electrode to reduce possible errors caused by the potentiostat at high frequencies. Before each individual impedance measurement, the electrode potential is held for 1 s; then ac probing signals are applied within the frequency range from 30 kHz to 5 Hz using 10 mV probing signal amplitude. The impedance spectra obtained at 1.6 V vs. RHE is selected for the further analysis and fitting, which are performed with a well-accepted physical model (the equivalent electric circuit is shown in Fig. 8b) describing the OER multistage mechanism, where at least one stage involving adsorbed intermediates is reversible. The as-obtained C_a is converted to ECSA via a specific adsorption capacitance (300±99 mF/cm$^2_{NiOx}$ for the as-used electrodeposited NiO_x thin-film), which is determined with the aid of AFM. This C_a method is a promising alternative technique that eliminates the convoluting side reactions in C_{DL}. Unfortunately, this method needs further improvement, because this C_a method has been only well demonstrated and reproduced at NiO_x thin-films; for other materials, the specific C_a, which converts C_a to ECSA, is unknown.

Except for advancing ECSA techniques, future challenges for ECSA measurement lie in some exceptional cases that the electrocatalysis is not a traditional surface process. For example, the $SrCoO_{3-\delta}$ oxide thickness involved during OER has been estimated to be as large as 14 nm;[46] in this bulky process, the quantification of active surface area is challenging. Finally, we remind that despite the pivotal role of determining the catalyst surface area in extracting specific activity, the best way to gain an insightful understanding of electrocatalysis is performing the activity analysis on a per site basis, i.e. TOF. Due to the difficulty in TOF estimation, now we have to rely on specific activity. The identification of the real active sites and how

to reliably quantify them are the ultimate goals in the electrocatalysis community.

7. Conclusions

This review introduces the experimental approaches for determining the surface area of metal oxide electrocatalysts. To rationalize why measuring the surface area of catalysts is crucial for electrocatalysis studies, we begin by analyzing the various metrics for estimating the electrocatalytic activity of a particular material. Through comparing the rationales of geometric activity, mass activity, TOF and specific activity, we validate the importance of surface-area-normalized activity (i.e. specific activity) to studies about the intrinsic chemistry of electrocatalyst. Then, we provide some general guidelines for measuring the ECSA. We rationalize the use of three-electrode cell, the selection of reference electrode, importance of gas inlet, and discuss the preparation of working electrode. Next, the experimental approaches for measuring the surface area of metal oxide catalysts are reviewed. To facilitate the understanding of ECSA measurement, we start from briefly describing the mechanisms of ECSA techniques for metal catalysts, where the ECSA measurement has been well demonstrated and applied in electrocatalysis studies. On the basis of metal catalysts, we focus on the priority of this review, i.e. the metal oxide catalysts, where the ECSA techniques are still limited and the surface area measurement currently has to rely on the non-electrochemistry methods, including AFM, BET and SEM/TEM analysis. For each method, we describe the detailed procedures to guide researchers to perform the experiment, discuss the rationales and limitations to help readers understand the applicability. Then, we give our recommendations on selecting a rational experimental approach for the surface area measurement of a particular metal oxide electrocatalyst. Lastly, we discuss the perspective to identify the future challenges that lie in the ECSA measurement and present an exemplary novel EIS technique that measures ECSA by adsorption capacitance.

Conflicts of interest

There are no conflicts to declare.

Acknowledgements

This work was supported by the Campus for Research Excellence and Technological Enterprise (CREATE) in Singapore and Singapore Ministry of Education Tier 2 Grant (MOE2017-T2-1-009). The authors thank the Facility for Analysis, Characterisation, Testing and Simulation (FACTS) in Nanyang Technological University for materials characterization.

Notes and references

1 M. B. Stevens, L. J. Enman, A. S. Batchellor, M. R. Cosby, A. E. Vise, C. D. M. Trang and S. W. Boettcher, *Chem. Mater.*, 2017, **29**, 120-140.

2 W. T. Hong, M. Risch, K. A. Stoerzinger, A. Grimaud, J. Suntivich and Y. Shao-Horn, *Energy Environ. Sci.*, 2015, **8**, 1404-1427.

3 K. A. Stoerzinger, M. Risch, B. Han and Y. Shao-Horn, *ACS Catal.*, 2015, **5**, 6021-6031.

4 M. Escudero-Escribano, A. Verdaguer-Casadevall, P. Malacrida, U. Grønbjerg, B. P. Knudsen, A. K. Jepsen, J. Rossmeisl, I. E. L. Stephens and I. Chorkendorff, *J. Am. Chem. Soc.*, 2012, **134**, 16476-16479.

5 T. J. Schmidt, H. A. Gasteiger, G. D. Stäb, P. M. Urban, D. M. Kolb and R. J. Behm, *J. Electrochem. Soc.*, 1998, **145**, 2354-2358.

6 C. L. Green and A. Kucernak, *J. Phys. Chem. B*, 2002, **106**, 1036-1047.

7 W. Sheng, M. Myint, J. G. Chen and Y. Yan, *Energy Environ. Sci.*, 2013, **6**, 1509-1512.

8 S. Trasatti and O. A. Petrii, *Pure Appl. Chem.*, 1991, **63**, 711-734.

9 M. Łukaszewski, M. Soszko and A. Czerwiński, *Int. J. Electrochem. Sci.*, 2016, **11**, 4442-4469.

10 E. Herrero, L. J. Buller and H. D. Abruña, *Chem. Rev.*, 2001, **101**, 1897-1930.

11 S. Jung, C. C. L. McCrory, I. M. Ferrer, J. C. Peters and T. F. Jaramillo, *J. Mater. Chem. A*, 2016, **4**, 3068-3076.

12 C. Wei and Z. J. Xu, *Small Methods*, 2018, 1800168.

13 J.-I. Jung, M. Risch, S. Park, M. G. Kim, G. Nam, H.-Y. Jeong, Y. Shao-Horn and J. Cho, *Energy Environ. Sci.*, 2016, **9**, 176-183.

14 R. Mohamed, X. Cheng, E. Fabbri, P. Levecque, R. Kötz, O. Conrad and T. J. Schmidt, *J. Electrochem. Soc.*, 2015, **162**, F579-F586.

15 J. H. Montoya, L. C. Seitz, P. Chakthranont, A. Vojvodic, T. F. Jaramillo and J. K. Nørskov, *Nat. Mater.*, 2016, **16**, 70-81.

16 F. J. Perez-Alonso, D. N. McCarthy, A. Nierhoff, P. Hernandez-Fernandez, C. Strebel, I. E. L. Stephens, J. H. Nielsen and I. Chorkendorff, *Angew. Chem., Int. Ed.*, 2012, **51**, 4641-4643.

17 M. Winter and R. J. Brodd, *Chem. Rev.*, 2004, **104**, 4245-4270.

18 H. A. Gasteiger and N. M. Marković, *Science*, 2009, **324**, 48-49.

19 K. A. Stoerzinger, L. Qiao, M. D. Biegalski and Y. Shao-Horn, *J. Phys. Chem. Lett.*, 2014, **5**, 1636-1641.

20 J. Suntivich, H. A. Gasteiger, N. Yabuuchi, H. Nakanishi, J. B. Goodenough and Y. Shao-Horn, *Nat. Chem.*, 2011, **3**, 546-550.

21 J. Suntivich, K. J. May, H. A. Gasteiger, J. B. Goodenough and Y. Shao-Horn, *Science*, 2011, **334**, 1383-1385.

22 C. Wei, R. R. Rao, J. Peng, B. Huang, I. E. L. Stephens, M. Risch, Z. J. Xu and Y. Shao-Horn, *Adv. Mater.*, 2019, 1806296.

23 K. A. Stoerzinger, W. Lü, C. Li, Ariando, T. Venkatesan and Y. Shao-Horn, *J. Phys. Chem. Lett.*, 2015, **6**, 1435-1440.

24 L. Trotochaud, J. K. Ranney, K. N. Williams and S. W. Boettcher, *J. Am. Chem. Soc.*, 2012, **134**, 17253-17261.

25 J. Zheng, W. Sheng, Z. Zhuang, B. Xu and Y. Yan, *Sci. Adv.*, 2016, **2**, e1501602-e1501609.

26 I. E. L. Stephens, A. S. Bondarenko, U. Gronbjerg, J. Rossmeisl and I. Chorkendorff, *Energy Environ. Sci.*, 2012, **5**, 6744-6762.

27 J. Y. C. Chen, J. T. Miller, J. B. Gerken and S. S. Stahl, *Energy Environ. Sci.*, 2014, **7**, 1382-1386.

28 Y. Zhou, S. Xi, J. Wang, S. Sun, C. Wei, Z. Feng, Y. Du and Z. J. Xu, *ACS Catal.*, 2018, **8**, 673-677.

29 Y. Gorlin and T. F. Jaramillo, *J. Am. Chem. Soc.*, 2010, **132**, 13612-13614.

30 J. Scholz, M. Risch, K. A. Stoerzinger, G. Wartner, Y. Shao-Horn and C. Jooss, *J. Phys. Chem. C*, 2016, **120**, 27746-27756.

31 L. Trotochaud, S. L. Young, J. K. Ranney and S. W. Boettcher, *J. Am. Chem. Soc.*, 2014, **136**, 6744-6753.

32 C. C. L. McCrory, S. Jung, J. C. Peters and T. F. Jaramillo, *J. Am. Chem. Soc.*, 2013, **135**, 16977-16987.

33 T. Poux, F. S. Napolskiy, T. Dintzer, G. Kéranguéven, S. Y. Istomin, G. A. Tsirlina, E. V. Antipov and E. R. Savinova, *Catal. Today*, 2012, **189**, 83-92.
34 E. Fabbri, R. Mohamed, P. Levecque, O. Conrad, R. Kötz and T. J. Schmidt, *ACS Catal.*, 2014, **4**, 1061-1070.
35 C. C. L. McCrory, S. Jung, I. M. Ferrer, S. M. Chatman, J. C. Peters and T. F. Jaramillo, *J. Am. Chem. Soc.*, 2015, **137**, 4347-4357.
36 Y. Yoon, B. Yan and Y. Surendranath, *J. Am. Chem. Soc.*, 2018, **140**, 2397-2400.
37 R. Tang, Y. Nie, J. K. Kawasaki, D.-Y. Kuo, G. Petretto, G. Hautier, G.-M. Rignanese, K. M. Shen, D. G. Schlom and J. Suntivich, *J. Mater. Chem. A*, 2016, **4**, 6831-6836.
38 L. C. Seitz, C. F. Dickens, K. Nishio, Y. Hikita, J. Montoya, A. Doyle, C. Kirk, A. Vojvodic, H. Y. Hwang, J. K. Norskov and T. F. Jaramillo, *Science*, 2016, **353**, 1011-1014.
39 K. A. Stoerzinger, M. Risch, J. Suntivich, W. M. Lu, J. Zhou, M. D. Biegalski, H. M. Christen, Ariando, T. Venkatesan and Y. Shao-Horn, *Energy Environ. Sci.*, 2013, **6**, 1582-1588.
40 S. Sun, H. Li and Z. J. Xu, *Joule*, 2018, **2**, 1024-1027.
41 Y. Zhou, Y. Du, S. Xi and Z. J. Xu, *Electrocatalysis*, 2017, **9**, 287-292.
42 C. Wei, Z. Feng, G. G. Scherer, J. Barber, Y. Shao-Horn and Z. J. Xu, *Adv. Mater.*, 2017, **29**, 1606800.
43 S. Zhou, X. Miao, X. Zhao, C. Ma, Y. Qiu, Z. Hu, J. Zhao, L. Shi and J. Zeng, *Nat. Commun.*, 2016, **7**, 11510-11516.
44 S. Yagi, I. Yamada, H. Tsukasaki, A. Seno, M. Murakami, H. Fujii, H. Chen, N. Umezawa, H. Abe, N. Nishiyama and S. Mori, *Nat. Commun.*, 2015, **6**, 8249-8254.
45 A. Grimaud, K. J. May, C. E. Carlton, Y. L. Lee, M. Risch, W. T. Hong, J. Zhou and Y. Shao-Horn, *Nat. Commun.*, 2013, **4**, 2439-2445.
46 A. Grimaud, O. Diaz-Morales, B. Han, W. T. Hong, Y.-L. Lee, L. Giordano, K. A. Stoerzinger, M. T. M. Koper and Y. Shao-Horn, *Nat. Chem.*, 2017, **9**, 457-465.
47 W. T. Hong, K. A. Stoerzinger, Y.-L. Lee, L. Giordano, A. Grimaud, A. M. Johnson, J. Hwang, E. J. Crumlin, W. Yang and Y. Shao-Horn, *Energy Environ. Sci.*, 2017, **10**, 2190-2200.
48 Y. Lee, J. Suntivich, K. J. May, E. E. Perry and Y. Shao-Horn, *J. Phys. Chem. Lett.*, 2012, **3**, 399-404.
49 P. J. Ferreira, G. J. la O', Y. Shao-Horn, D. Morgan, R. Makharia, S. Kocha and H. A. Gasteiger, *J. Electrochem. Soc.*, 2005, **152**, A2256-A2271.
50 S. Watzele and A. S. Bandarenka, *Electroanal.*, 2016, **28**, 2394-2399.